Polymer 49 (2008) 2014–2017

Contents lists available at ScienceDirect

Polymer

journal homepage: www.elsevier.com/locate/polymer

Polymer Communication

Hydrodynamic interaction and coalescence of two droplets under large step shear strains

Kenzo Okamoto [a,*], Shigenori Iwatsuki [b], Masaru Ishikawa [b], Masaoki Takahashi [c]

[a] Venture Laboratory, Kyoto Institute of Technology, Matsugasaki, Sakyo-ku, Kyoto 606-8585, Japan
[b] Department of Polymer Science and Engineering, Yamagata University, Jonan 4-3-16, Yonezawa, 992-8510, Japan
[c] Department of Macromolecular Science and Engineering, Kyoto Institute of Technology, Matsugasaki, Sakyo-ku, Kyoto 606-8585, Japan

ARTICLE INFO

Article history:
Received 9 October 2007
Received in revised form 19 February 2008
Accepted 2 March 2008
Available online 5 March 2008

Keywords:
Coalescence
Droplet
Hydrodynamic interaction

ABSTRACT

We observed change in distance between two droplets in each step after application of large multi-step shear strains. Experiments were performed using a sliding plate apparatus. Large step shear strains were applied to two polyisobutylene droplets in poly(dimethyl siloxane) matrix in the same plane between the plates. The distance between the two droplets decreases with increasing the total shear strain, which is given by the product of the step strain magnitude and the number of application of the step strains. The two droplets coalesce when the distance becomes less than the diameter of the droplets. The slope for plots of the distance versus the total strain is independent of the step strain magnitude. This indicates that the effect per unit strain on the distance is the same, irrespective of the strain magnitude. It is suggested that a stronger hydrodynamic interaction between the droplets is the main cause for the droplet approach.

1. Introduction

Interaction and coalescence of droplets are interesting subjects in polymer blends and interfacial phenomena. A large number of studies have been made in this field. One major method to investigate the interaction and coalescence of droplets is to observe morphology under transient shear flow and/or steady shear flow [1]. This kind of study is very useful to understand behaviors of droplets as an ensemble. On the other hand, another trend in recent studies is to investigate detailed shape of the interface during coalescence of droplets or lenses (droplets on a solid or a liquid substrate) [2–5]. Using high speed cameras, the latter investigations revealed dynamics of interface during coalescence. These two kinds of investigations dealt with two limiting cases of interaction and coalescence of droplets. However, interaction between droplets, which are close to each other and in deformed state, has not been investigated yet. This investigation is important to know how droplets approach and coalesce in flow fields.

In our previous study [6], we found that two droplets spontaneously approach under large step shear strains and coalesce after certain times of the application of the step strain. The driving force for the approach is considered to be hydrodynamic interaction between the droplets. However, details of the interaction were not clear, because experimental setup was not sufficient. In the present study, we used an apparatus by which observations from two directions are possible, i.e. from deformation-gradient and vorticity directions. This apparatus enables us to fix the droplets in the same shear plane and to apply step shear strains parallel to the line between the centers of the droplets. In addition, the distance between the parallel plates is relatively large so that the interaction from the plates can be minimized. The objective of the present study is to clarify the behavior of two droplets interacting under the large step shear strains. The criterion for the droplet coalescence is also investigated.

2. Experimental

We used polyisobutylene (PIB; Polyscience Co., Ltd.) as droplet and poly(dimethyl siloxane) (PDMS; Shinetsu Chemical Co., Ltd.) as matrix polymers. The zero shear viscosities of PIB, η_d, and PDMS, η_m, are $\eta_d = 95.5$ Pa s and $\eta_m = 1.08 \times 10^3$ Pa s at 23 °C, respectively. The interfacial tension Γ between these polymers are evaluated as $\Gamma = 3.1$ mN m^{-1} using the pendant droplet method. To apply large step shear strains and observe deformation of droplets, sliding plate geometry was adopted. Similar apparatus was used in our previous study [7]. The size of sliding plates (glass plates) with rectangular shape is 200 mm length, 50 mm width and 5 mm thickness. Using two glass spacers, the gap between the plates is kept at 2.7 mm or 5.0 mm during

* Corresponding author. Present address. School of Materials Science, Japan Advanced Institute of Science and Technology, Asahidai 1-1, Nomi, Ishikawa, 923-1292, Japan. Tel.: +81 761 51 1626; fax: +81 761 51 1149.
E-mail address: k-okamot@jaist.ac.jp (K. Okamoto).

0032-3861/$ – see front matter © 2008 Elsevier Ltd. All rights reserved.
doi:10.1016/j.polymer.2008.03.003

measurements. Two droplets are injected into the matrix using a micro-syringe in the middle of the gap so that the two droplets are on the same plane. By moving the lower glass plate parallel to its side and injecting the droplets, the droplets are arranged parallel to the side of the glass plates and the distance between the centers of the droplets, d_0, is adjusted. The radius of the droplet, r_0, was almost the same for the two droplets, ranging from 210–240 μm. The linear relaxation time τ_D of these droplets can be calculated using the Palierne theory [8,9] as

$$\tau_D = \frac{r_0\eta_m}{4\Gamma}\frac{(19K+16)(2K+3-2\phi(K-1))}{10(K+1)-2\phi(5K+2)},$$

where K is the viscosity ratio defined by $K=\eta_d/\eta_m$ and ϕ the volume fraction of droplets. Assuming the infinitely large matrix

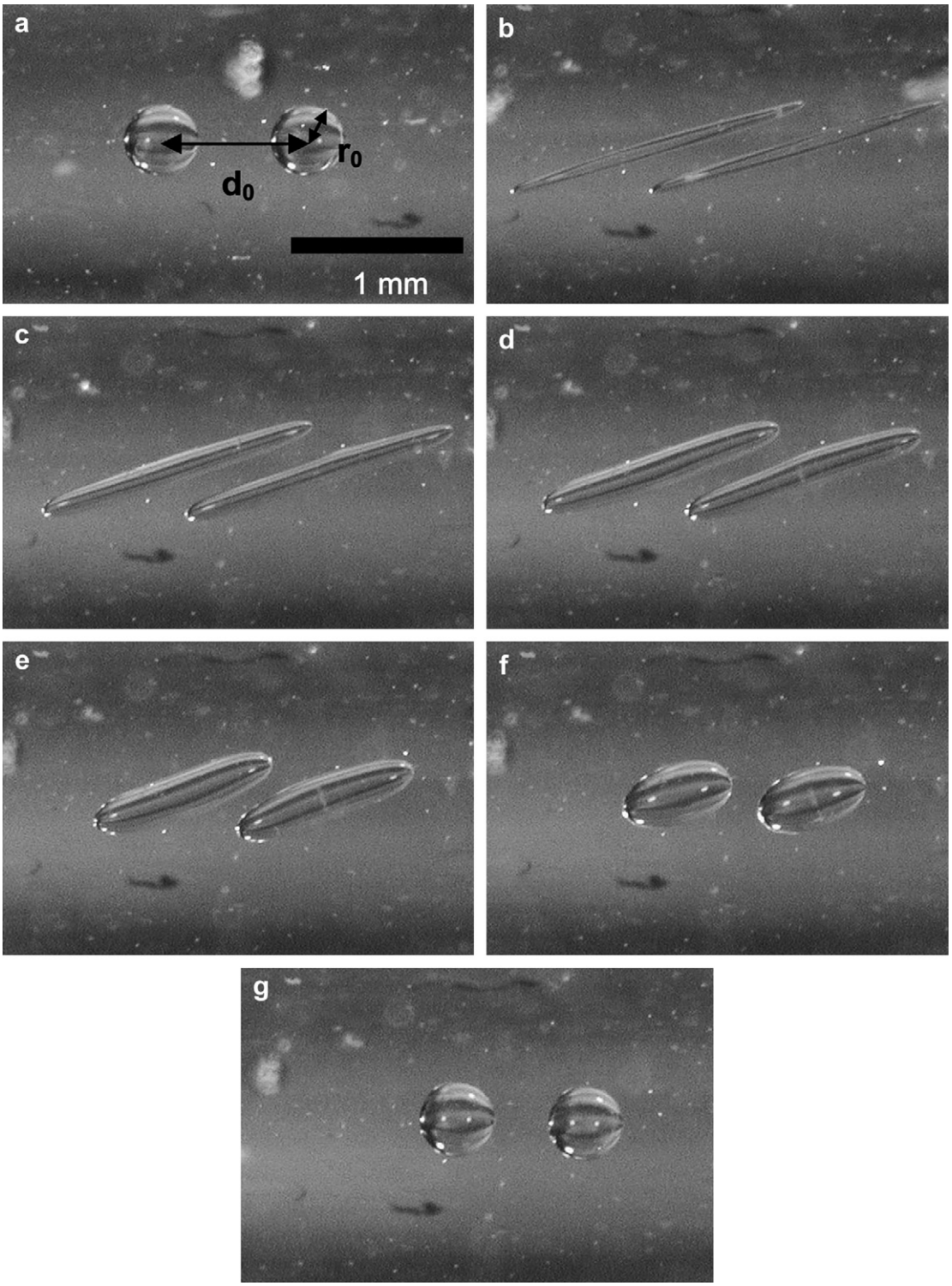

Fig. 1. Micrographs of two droplets observed from the vorticity direction (side view): (a) before application of shear deformation; (b) $t=0$ s (just after applying shear deformation); (c) $t=45$ s; (d) $t=90$ s; (e) $t=180$ s; (f) $t=360$ s and (g) $t=1200$ s (after recovery).

and setting $\phi = 0$ give $\tau_D = 94$–108 s for the droplets with $r_0 = 210$–240 μm.

The step shear strains were manually applied by moving the upper glass plate parallel to its side. The time necessary to apply the step strain γ is within 0.3 s for $\gamma = 4$ and 0.1 s for $\gamma = 1$. The shape and position of the droplets were observed from the deformation-gradient and vorticity directions using two stereo microscopes. For observation from the latter direction, a slide glass is fitted to the side of the glass plates. It was confirmed by observation from the deformation-gradient direction that the direction of the shear deformation was parallel to the line between the centers of the droplets. The time necessary to complete the recovery, $\tau_{complete}$, is almost the same as that for the recovery of the single droplet [6,7] when the coalescence does not occur, i.e., $\tau_{complete} \cong 300$ s for $\gamma = 1$ and $\tau_{complete} \cong 800$ s for $\gamma = 4$. When the droplets coalesce, $\tau_{complete}$ is somewhat longer than that for the single droplet [6]. After recovery of the deformed droplets, the upper glass plate is set back to the original position and the same shear deformation as the previous one was applied. These procedures were repeated until the two droplets coalesce.

3. Results

Fig. 1a–g shows micrographs of the two droplets observed from the vorticity direction (side view). The direction of deformation is horizontal and the direction of deformation-gradient is vertical in the micrographs. Before application of the shear deformation, two droplets are spherical with the radius r_0 and the distance d_0 (Fig. 1a). Just after application of the step shear strain $\gamma = 3$ ($t = 0$ s), the shape of the droplets is close to ellipsoid given by affine deformation assumption (Fig. 1b). Deformation of the droplets recovers owing to the interfacial tension between the droplet and the matrix phases, and the length of the major axis of droplets decreases (Fig. 1c–e). It should be noted that shape of the droplet is not symmetric in these micrographs. Fig. 1c–e shows bending or even sigmoidal shape of droplets, which are not observed for a single isolated droplet [7]. This asymmetric shape might result from interaction between the two droplets. At $t = 360$ s (Fig. 1f), the droplets further retract and the shape of the droplets become ellipsoid of revolution. Though asymmetric shape of the droplets is not prominent in this stage, angle between the major axis of the droplets and shear flow direction, θ, is slightly less than that at $t = 0$ s as a result of the bending of the droplets during the retraction. It can be seen that d_0 after the recovery (Fig. 1g) is smaller than that before deformation (Fig. 1a). This indicates that attractive interaction acts between the droplets during the shape recovery.

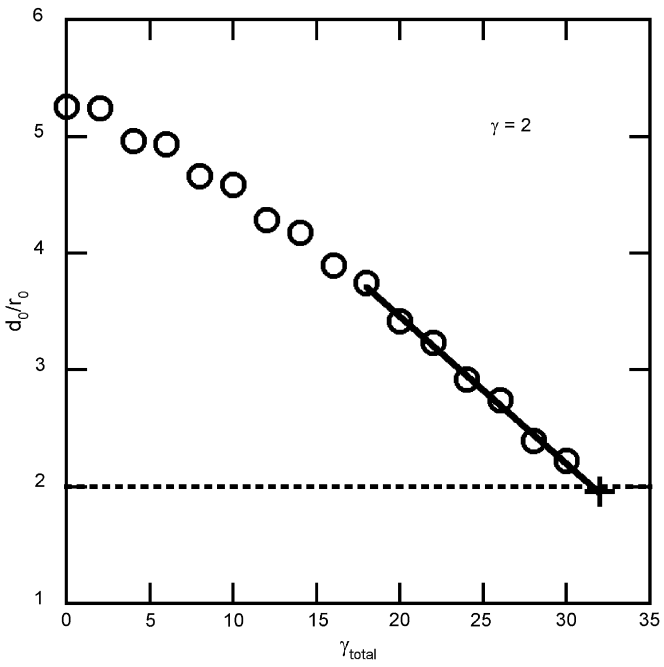

Fig. 2. Plots of d_0/r_0 versus γ_{total} at $\gamma = 2$ (open circles). The solid line indicates the least square fit with the experimental data. The cross-symbol shows the extrapolation of the least square calculation to $\gamma_{total} = \gamma_{coal}$.

Table 1
The slope of the plots of d_0/r_0 versus γ_{total} at $d_0/r_0 < 3.8$, $\Delta(d_0/r_0)/\Delta\gamma_{total}$, and the total strain at the coalescence of the droplets $(d_0/r_0)_{coal}$, for various step strains γ

γ	$\Delta(d_0/r_0)/\Delta\gamma_{total}$	$(d_0/r_0)_{coal}$
2	−0.12	1.92
3	−0.14	1.91
4	−0.13	1.77

Fig. 2 shows the normalized distance d_0/r_0 as a function of the total strain γ_{total} at $\gamma = 3$, where γ_{total} is given by

$$\gamma_{total} = n\gamma. \quad (1)$$

Here, n is the number of step shear strains applied. In Fig. 2, open circles indicate experimental data for d_0/r_0. The distance d_0/r_0 decreases with increasing γ_{total} or n. At $d_0/r_0 < 3.8$, d_0/r_0 is proportional to γ_{total}, where the proportionality constant is negative. The solid line in the figure represents calculated result, which is determined by the least square method at $d_0/r_0 < 3.8$. The slope of the line, $\Delta(d_0/r_0)/\Delta\gamma_{total}$, is −0.127. A cross-symbol indicates extrapolation of the calculated result to γ_{total} at the coalescence, γ_{coal}. In Fig. 2, γ_{coal} is given by $\gamma_{coal} = 32$. The extrapolated value of d_0/r_0 to γ_{coal} is $d_0/r_0 = 1.94$. We refer to this extrapolated value as $(d_0/r_0)_{coal}$.

Table 1 summarizes $\Delta(d_0/r_0)/\Delta\gamma_{total}$ and $(d_0/r_0)_{coal}$ for $\gamma = 2$, 3 and 4. In Table 1, $\Delta(d_0/r_0)/\Delta\gamma_{total}$ is almost the same and $(d_0/r_0)_{coal}$ is slightly smaller than 2 for $\gamma = 2$, 3 and 4. This means that change in d_0/r_0 per unit shear strain is the same at $\gamma = 2$, 3 and 4. Moreover, the droplets coalesce if d_0/r_0 after recovery is less than 2, i.e., if the droplets overlap each other after recovery.

4. Discussion

A part of the experimental results may be explained by hydrodynamic interaction between the droplets. Fig. 3 shows the calculated flow field in the matrix at $t = 0$, in which origin of arrows indicates a point in the matrix and length and direction of the

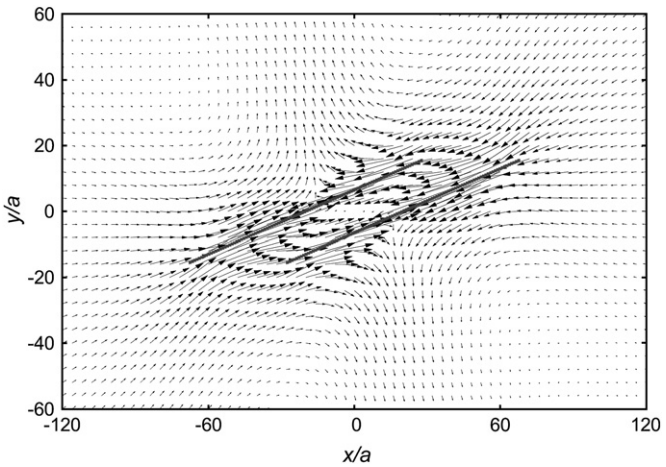

Fig. 3. Flow field in the matrix at $t = 0$ calculated based on a hydrodynamic interaction model [10]. Solid lines represent the droplets.

arrows show velocity vector of the flow at the point. The calculation was performed based on a simple model which considers hydrodynamic interaction between the two droplets. In this model, the droplets are represented by a number of rigid spheres with radius a, which aligns on a line with the orientation angle θ to x axis, and the retraction of droplets is driven by harmonic potentials which act on the rigid spheres. The flow field in the matrix is calculated using the Oseen's equation. Detail of the model will be described in the following paper [10].

In Fig. 3, the number of the rigid spheres for one droplet is hundred, and coordinates of centers of mass for the rigid spheres are $(x,y) = (-20a,0)$ and $(x,y) = (20a,0)$, respectively. Orientation angle θ is given by $\theta = \pi/10$. The rigid spheres, which represent the droplets, are indicated by closed squares (although difficult to see at low magnification). Fig. 3 shows that lower part of the left droplet experiences flow from left to right while upper part of the same droplet experiences flow from right to left. In the vicinity of the left droplet, summation of the flow seems to be from left to right. In the vicinity of the right droplet, summation of flow in the matrix seems to be from right to left. As a result, the droplets move toward the other ones owing to the flow of the matrix. Actually, the result of the calculation indicates that distance between the centers of mass of the rigid spheres for each droplet decreases with increasing time. This strongly indicates that the experimental results in the present study are caused by the hydrodynamic interaction between the droplets. It should be noted that the above model does not consider increase of minor axis of the droplets, which can cause repulsive interaction opposite to the above consideration. However, increase of length of the minor axis is much smaller than decrease of length of the major axis. This may be the reason why the above model explains the experimental results well.

Very recently we found that time evolution of axes (retraction) for isolated droplet with spheroidal shape is independent of γ, when time is reduced by $(t - t_S)/\tau_D$, where τ_D is the linear relaxation time of the droplet and t_S is a starting time for the spheroidal shape [11]. We showed that the stress calculated by using the interface tensor [12,13] can be reduced similarly and a normalized stress is expressed by a single curve independent of γ [11]. Even if contribution from the interface velocity [14,15] is considered, the normalized stress relaxation curves at the last stage are independent of γ [16]. However, experimental data of the stress relaxation for polyisobutylene/poly(dimethyl siloxane) blends exhibit significant γ-dependence in the reduced plots [11,16]. This indicates that effects of other droplets in blends cannot be neglected at all. One of the effects is considered to be the hydrodynamic interaction as the present experimental results show. Actually, d_0/r_0 for 20 vol% of droplets in the blends was calculated as $d_0/r_0 = 2.8$ assuming simple cubic lattice. This distance is much smaller than that of the attractive interaction range between two droplets, which is more than 5 as shown in Fig. 2. The effects of hydrodynamic interaction on the stress relaxation of real blends clearly need further investigations.

5. Conclusions

Dependence of the distance between two droplets on the applied step shear strains was determined by direct observation of the droplets under large strains. The distance decreases with increasing the total strain applied, and the droplets coalesce when the distance is less than the droplet diameter. Calculation based on the model [10] indicates that the decrease of the distance is caused by the hydrodynamic interaction between the two droplets. The hydrodynamic interaction is considered to be one of the causes for the strain dependence of the normalized stress relaxation curves found very recently [11,16].

Acknowledgments

This work was supported by a grant from Izumi Science and Technology Foundation and a Grant-in-Aid for Scientific Research (B) No. 18350119 from the Japan Society for the Promotion of Science (JSPS). Technical assistance of Mr. Masaaki Konno and valuable discussions with Prof. Kunihiro Osaki and Prof. Toshikazu Takigawa are greatly appreciated.

References

[1] For example, Minale M, Moldenaers P, Mewis J. Macromolecules 1997;30:5470–5; Burkhart BE, Gopalkrishnan PV, Hudson SD, Jamieson AM, Rother MA, Davis RH. Phys Rev Lett 2001;87:098304;
Takahashi Y, Kato T. Nihon Reoroji Gakkaishi (J Soc Rheol Japan) 2005;33:37–9 [Downloadable from <http://www.jstage.jst.go.jp/browse/rheology/33/1/_contents>];
Caserta S, Simeone M, Guido S. Rheol Acta 2006;45:505–12.
[2] Menchaca-Rocha A, Martinez-Davalos A, Nunez R. Phys Rev E 2001;63:046309.
[3] Chen N, Kuhl T, Tadmor R, Lin Q, Israelachvili J. Phys Rev Lett 2004;92:024501.
[4] Aarts DGAL, Lekkerkerker HNW, Guo H, Wegdam GH, Bonn D. Phys Rev Lett 2005;95:164503.
[5] Burton JC, Taborek P. Phys Rev Lett 2007;89:224502.
[6] Okamoto K, Tamura R, Ishikawa M. Nihon Reoroji Gakkaishi (J Soc Rheol Japan) 2002;30:45–8. Downloadable from <http://www.jstage.jst.go.jp/browse/rheology/30/1/_contents>.
[7] Yamane H, Takahashi M, Hayashi R, Okamoto K, Kashihara H, Masuda T. J Rheol 1998;42:567–80.
[8] Palierne JF. Rheol Acta 1990;29:204–14.
[9] Graebling D, Muller R, Palierne JF. Macromolecules 1993;26:320–9.
[10] Okamoto K, Osaki K, Takahashi M, Yamaguchi M, in preparation.
[11] Takahashi M, Okamoto K. Nihon Reoroji Gakkaishi (J Soc Rheol Japan) 2007;35:199–205. Downloadable from <http://www.jstage.jst.go.jp/browse/rheology/35/4/_contents>.
[12] Onuki A. Phys Rev A 1987;35:5149–55.
[13] Doi M, Ohta T. J Chem Phys 1991;95:1242–8.
[14] Batchelor GK. J Fluid Mech 1970;41:545–70.
[15] Mellema J, Willemse WM. Physica 1983;A122:286–312.
[16] Okamoto K, Takahashi M. Nihon Reoroji Gakkaishi (J Soc Rheol Japan) 2008;36:43–9. Downloadable from <http://www.jstage.jst.go.jp/browse/rheology/36/1/_contents>.